Axonal filopodial asymmetry induced by synaptic target

Pan P. Li, Cheng Chen*, Chi-Wai Lee†, Raghavan Madhavan, and H. Benjamin Peng
Division of Life Science, State Key Laboratory of Molecular Neuroscience, The Hong Kong University of Science and Technology, Clear Water Bay, Hong Kong, China

ABSTRACT **During vertebrate neuromuscular junction (NMJ) assembly, motor axons and their muscle targets exchange short-range signals that regulate the subsequent steps of presynaptic and postsynaptic specialization. We report here that this interaction is in part mediated by axonal filopodia extended preferentially by cultured *Xenopus* spinal neurons toward their muscle targets. Immunoblotting and labeling experiments showed that basic fibroblast growth factor (bFGF) was expressed by muscle and associated with the cell surface, and treatment of cultured spinal neurons with recombinant bFGF nearly doubled the normal density of filopodia in neurites. This effect of bFGF was abolished by SU5402, a selective inhibitor of FGF-receptor 1 (FGFR1), and forced expression of wild-type or dominant-negative FGFR1 in neurons enhanced or suppressed the assembly of filopodia, respectively. Significantly, in nerve–muscle cocultures, knocking down bFGF in muscle decreased both the asymmetric extension of filopodia by axons toward muscle and the assembly of NMJs. In addition, neurons expressing dominant-negative FGFR1 less effectively triggered the aggregation of muscle acetylcholine receptors at innervation sites than did control neurons. These results suggest that bFGF activation of neuronal FGFR1 generates filopodial processes in neurons that promote nerve–muscle interaction and facilitate NMJ establishment.**

Monitoring Editor
Thomas D. Pollard
Yale University

Received: Mar 9, 2011
Revised: May 4, 2011
Accepted: May 13, 2011

INTRODUCTION

Synapses promote neuronal communication by positioning neurotransmitter release and detection sites near each other. At the vertebrate neuromuscular junction (NMJ), for example, the presynaptic motor terminal is enriched in synaptic vesicles (SVs) that store and release acetylcholine, and the apposing postsynaptic muscle membrane is packed with ~10,000 acetylcholine receptors (AChRs) per μm^2 (Fertuck and Salpeter, 1976). Given this arrangement, AChR opening and postsynaptic depolarization faithfully follow every presynaptic action potential to cause muscle contraction. Thus, in studies on NMJ assembly, much effort has been devoted to investigating the presynaptic accumulation of SVs and postsynaptic clustering of AChRs (Sanes and Lichtman, 2001).

According to the current view, synaptic AChR aggregation and stabilization occur in response to the activation of the muscle receptor tyrosine kinase MuSK, which is stimulated by the nerve-secreted heparan sulfate proteoglycan (HSPG) agrin and the transmembrane protein Lrp4 (Sanes and Lichtman, 2001; Madhavan and Peng, 2005; Kummer *et al.*, 2006; Kim *et al.*, 2008; Zhang *et al.*, 2008). The molecular mechanism that leads to presynaptic development is less well characterized, although a number of factors have been shown to contribute to this process. These include Schwann cell–derived factors (Feng and Ko, 2008), cell adhesion molecules (Gerrow and El-Husseini, 2006), extracellular matrix (Nishimune *et al.*, 2004), and growth factors (Dai and Peng, 1995, 1998; Fitzsimonds and Poo, 1998; Fox and Umemori, 2006; Feng and Ko, 2008).

In the establishment of central synapses, cell-to-cell contacts mediated by dendritic filopodial processes have been shown to play a major role (Heiman and Shaham, 2010). Similarly, filopodia generated by postsynaptic muscle cells, termed myopodia, are involved in NMJ formation (Ritzenthaler *et al.*, 2000; Uhm *et al.*, 2001;

This article was published online ahead of print in MBoC in Press (http://www.molbiolcell.org/cgi/doi/10.1091/mbc.E11-03-0198) on May 25, 2011.

Present addresses: *Department of Medicine, University of Hong Kong, Pokfulam, Hong Kong, China; †Department of Cell Biology, Emory University School of Medicine, Atlanta, GA 30303.

Address correspondence to: H. Benjamin Peng (penghb@ust.hk).

Abbreviations used: AChR, acetylcholine receptor; AI, asymmetry index; bFGF, basic fibroblast growth factor; FGFR1, fibroblast growth factor receptor 1; MO, morpholino oligonucleotide; NMJ, neuromuscular junction.

Madhavan *et al.*, 2006). Myopodia facilitate adhesive interactions between the nerve and muscle and promote synaptogenesis. In vertebrate muscle, myopodia are formed in response to neural agrin, and blocking their assembly has been found to hinder the development of AChR clusters at nerve–muscle contacts (Uhm *et al.*, 2001; Madhavan *et al.*, 2006). In our previous study using *Xenopus* nerve–muscle cocultures it was noted that spinal axons also extended filopodia that make contacts with myopodia and muscle cells (Madhavan *et al.*, 2006), but it has remained unclear whether factors from muscle induce neuronal filopodia and whether neuronal filopodia influence the synaptogenic interactions between nerve and muscle.

In this study we investigated the role of the muscle target in filopodial induction in axons during the early stages of NMJ formation. We report that axonal filopodia are preferentially extended toward muscle and that this process involves muscle-derived basic fibroblast growth factor (bFGF), a molecule previously shown to induce presynaptic specialization when locally applied via beads (Dai and Peng, 1995; Lee and Peng, 2006). Our results further suggest that this asymmetric generation of filopodia in axons facilitates NMJ establishment.

RESULTS

Preferential protrusion of axonal filopodia toward muscle target

Filopodial processes in growth cones enable a growing neurite to detect environmental cues (Gallo and Letourneau, 2004). Filopodia also develop along the shaft of growing axons, as seen in the example in Figure 1A, which shows the axon of a *Xenopus* embryonic spinal neuron cultured in the absence of muscle target. We found that these axonal filopodia varied in length from a few to more than 20 µm (Figure 1) and were quite dynamic, extending out and retracting within minutes. In addition, as also shown in Figure 1, these processes were often associated with varicosities along the axon. To investigate muscle's influence on the formation and stabilization of neuronal filopodia, we examined live cocultures of *Xenopus* spinal neurons and myotomal muscle cells. Axons approaching muscle cells were identified, and the extension of filopodia by these axons was compared with that in axons in pure nerve cultures. In pure nerve cultures, the density of filopodia in a stretch of axon was approximately equal on either side (Figure 1A). In contrast, in the nerve–muscle cocultures, axons near muscle cells had significantly more filopodia along their muscle-facing side than on the muscle-free side (Figure 1B). To quantify this difference, filopodia were counted in axon segments ≤30 µm from the edge of muscle cells and in axon segments selected randomly in pure nerve cultures. From this we calculated an asymmetry index (AI) (Figure 1C), the values of which positive if more filopodia are disposed toward muscle and negative if the opposite is true; thus an AI value of +1 or −1 represents the protrusion of all filopodia from the muscle-facing or muscle-free side of axons, respectively, and an AI of 0 signifies equal filopodial extension by both sides. In pure nerve cultures, the sidedness of filopodial origin was defined arbitrarily. On the basis of data pooled from three separate cultures, the filopodial density (number of filopodia per 10-µm axonal length) in nerve–muscle cocultures was more than twice the value in pure nerve cultures (Figure 1J). Filopodia emanated equally on either side of the axon in pure nerve cultures. In cocultures, however, many more filopodia were seen on the side facing the muscle target (Figure 1J). The AI of filopodial distribution was calculated to be ~0.07 for axons in pure neuron cultures, whereas in cocultures this value reached 0.6 (Figure 1K), thus indicating high asymmetry in the formation of these cellular processes toward muscle target.

Time-lapse imaging was next carried out on axons that approached muscle cells in cocultures to examine filopodial formation and retraction. These recordings showed that ~16% of filopodia were newly formed on the muscle-facing side as compared with ~7% on the muscle-free side per 10-min period (Figure 1L, open bars). However, these numbers showed large variation and were not statistically significant. On the other hand, the stability of filopodia on the two sides of the axon showed highly significant difference. Those on the muscle-facing side were retracted much less often than those on the muscle-free side over a 10-min time interval (Figure 1, D–I). Data from several axon–muscle pairs revealed that neuronal filopodia extending toward muscle were four times more stable than those protruding away (Figure 1L, hatched bars). These results show that the presence of muscle promotes both the formation and the stabilization of axonal filopodia in an asymmetric manner toward the target.

Expression of bFGF by *Xenopus* muscle and its concentration at AChR clusters

The foregoing results suggested that neuronal filopodia were induced and stabilized by muscle cells. Thus molecules associated with the surface of muscle cells were examined. Among muscle surface-bound molecules, a member of the FGF family, bFGF, was a prominent candidate since it is sequestered there through binding to HSPGs and is known to induce presynaptic differentiation in *Xenopus* motor neurons (Dai and Peng, 1995; Lee and Peng, 2008). To test whether muscle-associated bFGF can function as a regulator of filopodial assembly in spinal neurons, we first examined the expression and localization of bFGF in *Xenopus* muscle. In extracts of *Xenopus* embryonic muscle, a single full-length bFGF protein band was detected by an anti-bFGF antibody (Figure 2A, top blot). The same antibody also stained exogenous bFGF in extracts of HEK293 cells transfected with a cDNA encoding mouse bFGF (positive control) but not green fluorescent protein (GFP) (negative control). In our immunoblots more bFGF was detected in extracts of muscle tissue than of neural tubes (Figure 2A, top blot); in the example shown total protein amounts in extracts of *Xenopus* muscle, neural tubes, whole embryos, and HEK293 cells can be compared by anti-tubulin antibody staining (bottom blot).

To examine whether bFGF was associated with the muscle surface, immunofluorescent labeling was carried out on live muscle cultures and 1-d-old nerve–muscle cocultures. Cultures were first labeled with rhodamine-conjugated α-bungarotoxin (R-BTX) to mark muscle AChR clusters and then with control (Figure 2, B–D), anti-bFGF (Figure 2, E–J), and fluorescein isothiocyanate (FITC)–linked secondary antibodies (Figure 2, B–J). Anti-bFGF staining was present on the muscle surface, and the labeling was especially strong at AChR clusters that developed spontaneously in pure muscle cultures (Figure 2, E–G) and those that were induced at innervation sites in cocultures (Figure 2, H–J). In accord with our immunoblotting results and demonstrating specificity, anti-bFGF antibody labeled neurons poorly (Figure 2A), and several control antibodies (including one against GFP; Figure 2, B–D) stained neither muscle cells nor neurons.

These results indicated the expression of bFGF by *Xenopus* muscle cells and placed bFGF in a position suitable for regulating filopodial growth in *Xenopus* spinal neurons.

Effect of exogenous bFGF on filopodial formation

Can bFGF regulate the development of filopodia in spinal neurons? To address this, pure nerve cultures were incubated overnight in

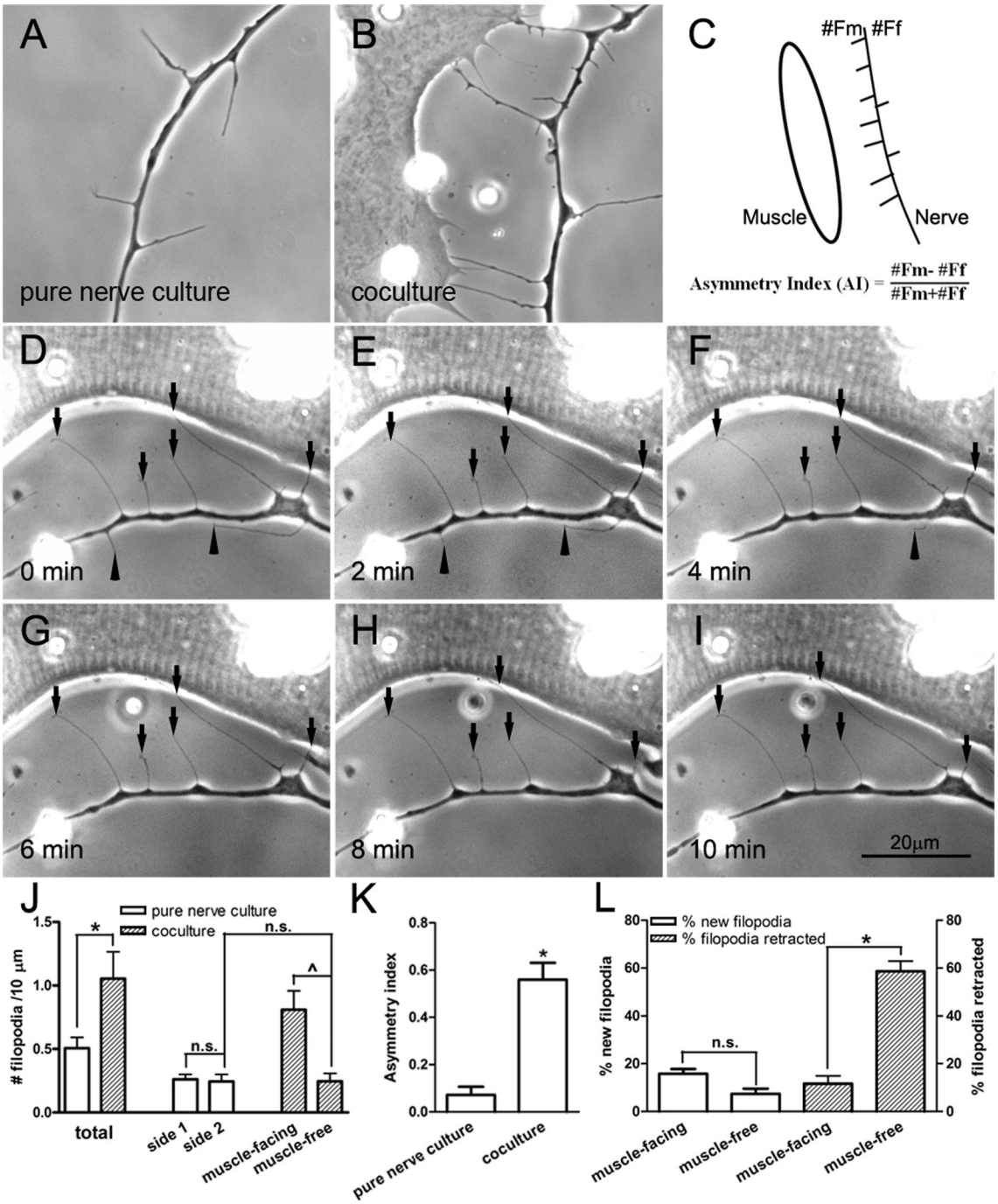

FIGURE 1: Axonal filopodia generated by *Xenopus* spinal neurons. In the absence of muscle target, filopodia were generated on either side of the axon with equal frequency (A). However, when a muscle cell was nearby (cell on the left in B), more filopodia were extended toward the target. (C) This difference was quantified by calculating the AI by scoring filopodia from the muscle-facing side (#Fm) vs. those on muscle-free side (#Ff) along axon segments within 30 μm from muscle. (D–I) Time-lapse recording of filopodia near a muscle cell. Muscle-facing filopodia were more stable (pointed out by arrows) than those on the opposite side (arrowheads pointing to filopodia that disappeared with time). (J) Filopodial density determined by scoring them along the length of the axon. The presence of the muscle target caused a large increase in their total density. Most of this increase was seen asymmetrically along the muscle-facing side of the axon. No asymmetry was seen along axons in pure nerve cultures without muscle target. Fifty-three axons from pure nerve culture and 42 axons from nerve–muscle cocultures were counted. (K) AI calculated from axonal segments in pure nerve cultures and nerve–muscle cocultures (22 axons from pure nerve cultures and 26 from nerve–muscle cocultures). The presence of muscle caused highly asymmetric filopodia disposition, with an AI value of 0.56 ± 0.07. (L) The formation (open bars) and retraction (hatched bars) of axonal filopodia in cocultures. On the muscle-facing side of the axon, more new filopodia were formed than on the muscle-free side. However, the major difference was seen in the stability of filopodia on the muscle-facing side. This is shown by the much lower rate of retraction during a 10-min period. Nineteen nerve–muscle cocultures were scored. In J–L, the mean ± SEM in each case is plotted, *$p < 0.05$ (Student's *t* test).

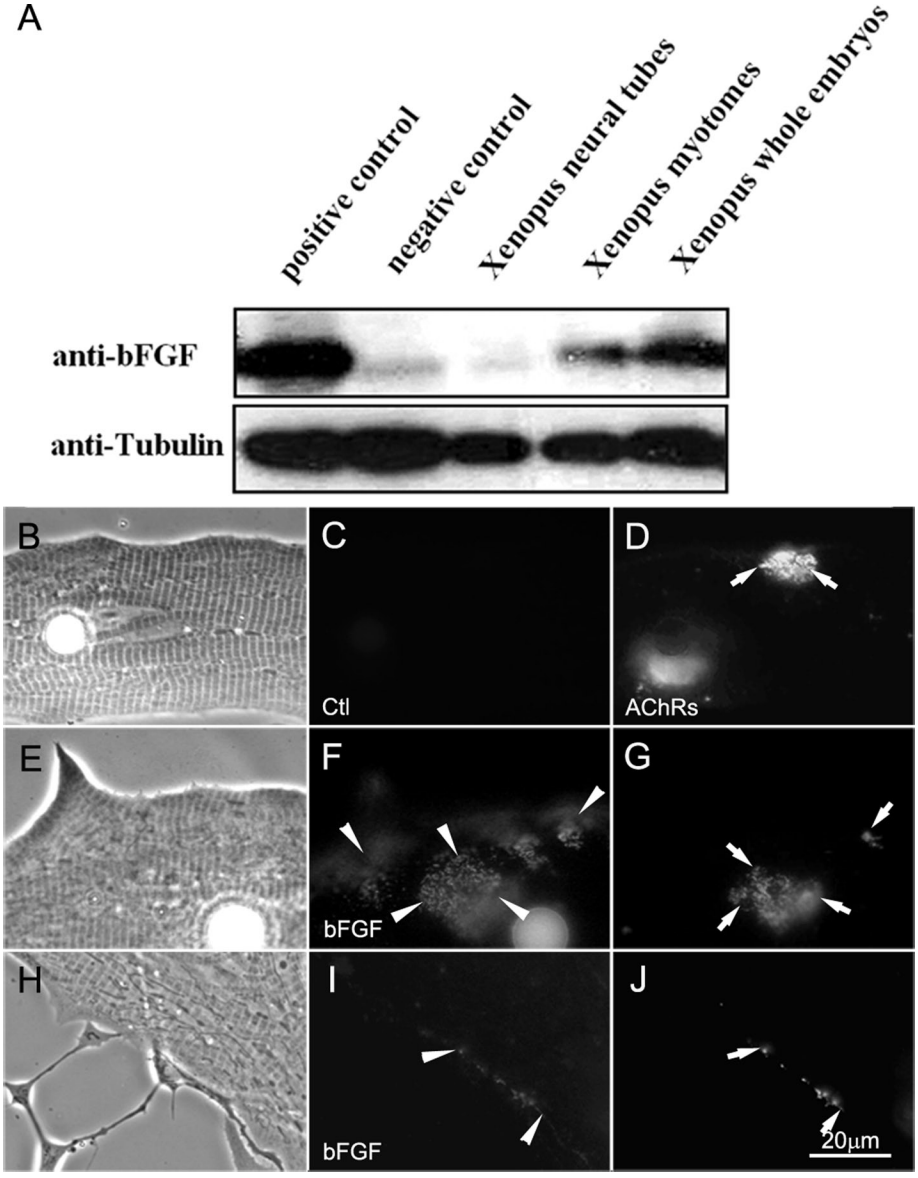

FIGURE 2: The expression of bFGF in *Xenopus* embryos. (A) Western blots of *Xenopus* embryonic extracts were probed for bFGF. The positive and negative controls used (first two lanes) were extracts of HEK293 cells overexpressing bFGF and GFP, respectively. The other three lanes contained extracts from *Xenopus* neural tubes, myotomal muscle, and whole embryos. Tubulin was used as protein loading control. *Xenopus* myotomal muscle expressed a higher level of bFGF than neural tubes. (B–J) Localization of bFGF in *Xenopus* myotomal muscle cells in culture. Cells were labeled live with anti-bFGF (F, I) or anti-GFP (control, C) and FITC-conjugated secondary antibodies. R-BTX labeling (D, G, J) was used to visualize AChR clusters. Although the muscle cell showed an overall labeling for bFGF, this growth factor was more concentrated at AChR clusters in muscle (E–G) and at developing NMJs in nerve–muscle cocultures (H–J).

control medium or in medium that contained recombinant human bFGF (100 ng/ml). In these cultures more filopodia were detected in bFGF-treated neurons than in control neurons (Figure 3, A and B). Axon segments were randomly chosen from control and bFGF-stimulated cultures, and all filopodia present in the segments were counted. Calculation of filopodial densities (number of filopodia/10 μm) showed that nearly twice as many filopodia were present in bFGF-treated neurons as in control neurons (Figure 3J, open bars). Control molecules such as neurotrophins, which are unrelated to bFGF, failed to enhance filopodial density in spinal neurons, although the neurotrophins promoted neuronal survival as expected (unpublished data). Moreover, addition of the FGFR1-selective inhibitor SU5402 (20 μM) to neuronal cultures abolished bFGF's ability to induce filopodia (Figure 3, C and J, shaded bars); at the concentration used, however, SU5402 did not significantly affect filopodial assembly in neurons in the absence of bFGF (Figure 3J). These results supported the conclusion that bFGF treatment stimulated filopodial growth in spinal neurons, as it does in CNS neurons (Szebenyi *et al.*, 2001), and further suggested that bFGF acted via FGFR1 in spinal neurons.

Effect of FGFR1 overexpression on filopodial formation

To directly investigate the possible involvement of FGFR1 signaling in the induction of neuronal filopodia, active and inactive forms of FGFR1 were introduced into spinal neurons (Figure 3). We used *Xenopus* wild-type FGFR1 (WT-FGFR1) and a mutant form of FGFR1 with its intracellular domain truncated (TR-FGFR1). Constructs encoding these proteins were first transfected into HEK293T cells, and biochemical assays were used to confirm that WT-FGFR1 could be tyrosine phosphorylated, whereas no phosphorylation of TR-FGFR1 was detected in the absence or presence of bFGF (unpublished data).

Xenopus embryos at the two-cell stage were injected with mRNAs encoding WT-FGFR1 or TR-FGFR1 mixed with GFP mRNA, which was used by itself as a control. Examination of spinal neurons isolated from these embryos at stage 20–22 showed that WT-FGFR1 neurons (Figure 3, E and E′) had more filopodia than GFP neurons (Figure 3, D and D′), whereas TR-FGFR1 neurons had fewer filopodia (Figure 3, F and F′). Quantification showed that the expression of WT-FGFR1 increased the density of neuronal filopodia by ~90% relative to control (Figure 3K) and that of TR-FGFR1 reduced filopodial formation by ~35%. Moreover, in these neurons, unlike in control neurons, exogenous bFGF did not further alter filopodial densities (unpublished data), supporting the notion that FGFR1 mediates bFGF-dependent filopodial enhancement. In the course of these experiments we also noted that embryos expressing high levels of TR-FGFR1 showed abnormal development, exhibiting open dorsal part (P.P.L. and H.B.P., unpublished observations), a phenotype consistent with the previously described function of FGFR1 activity in dorsal closure during embryonic development (Amaya *et al.*, 1991; Kusakabe *et al.*, 2001). Furthermore, in spinal neurons overexpressing WT-FGFR1, excess filopodial assembly was blocked by the addition of SU5402 (Figure 3, H and H′), which did not affect filopodial formation in TR-FGFR1 neurons (Figure 3, I and I′) and GFP neurons

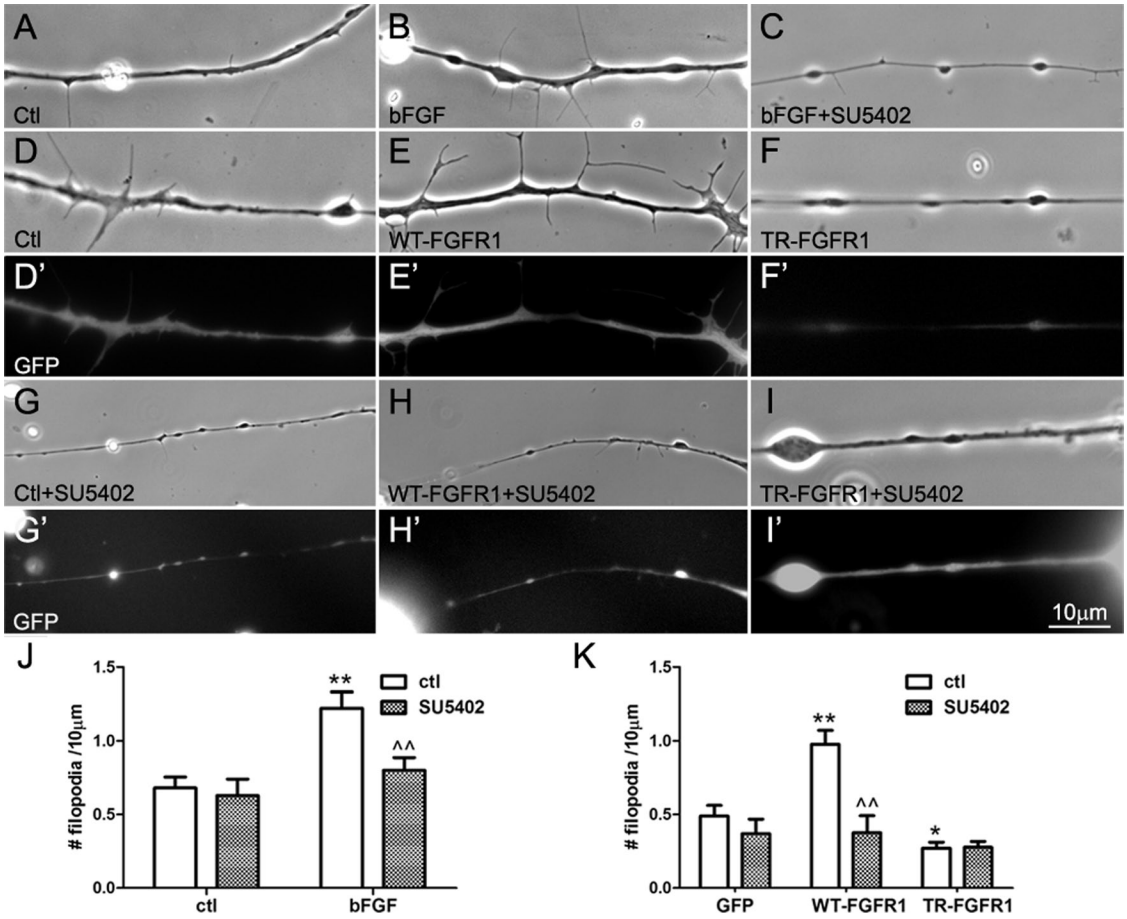

FIGURE 3: The effect of bFGF/FGFR1 on axonal filopodial density. Spinal neurons were incubated in control medium (A) or in medium containing bFGF (100 ng/ml) (B) or bFGF plus the FGFR1 inhibitor SU5402 (20 μM) (C). Neurite segments were randomly selected, and all the filopodia present in them were counted to calculate filopodial density (number of filopodia/10 μm). More filopodia were found in neurons treated with bFGF than in control neurons, but this change was absent when SU5402 was added with bFGF; by itself SU5402 did not affect the basal filopodial assembly in neurons (J). (D, D′ to I, I′). To test FGFR1's role in the induction of neuronal filopodia, spinal neurons were cultured from *Xenopus* embryos injected with mRNAs encoding GFP (D, D′ and G, G′), WT-FGFR1 and GFP (E, E′ and H, H′), or TR-FGFR1 and GFP (F, F′ and I, I′). Neurons were examined in phase contrast for filopodia, and GFP fluorescence confirmed the expression of exogenous proteins in neurons. In WT-FGFR1 neurons more filopodia were found than in control GFP neurons (E vs. D), but in TR-FGFR1 neurons fewer filopodia were detected than in GFP neurons (F vs. D). The enhancement of filopodial growth in WT-FGFR1 neurons was blocked by the addition of SU5402 (H), but SU5402 did not significantly affect the already low filopodial density in TR-FGFR1 neurons (I) and only slightly reduced filopodia in GFP neurons (G). Filopodial densities in neurons expressing the exogenous proteins are shown in K (mean ± SEM; *t* test, *$p < 0.05$ and **$p < 0.01$, compared with control; ^^$p < 0.01$, compared with no SU5402 treatment).

(Figure 3, G and G′). These effects of FGFR1 proteins and SU5402, quantified as filopodial densities in Figure 3K (shaded bars), suggested that enhanced activation FGFR1 in spinal neurons increased the formation of filopodia.

Regulation of filopodial asymmetry by bFGF-FGFR1 signaling

Spinal neurons expressing wild-type and mutant FGFR1 proteins were next cocultured with normal muscle cells. In the axons of these neurons that approached muscle the AI of filopodial distribution was calculated as before. Here, as in pure nerve cultures, the density of filopodia in WT-FGFR1 neurons was higher than in control GFP neurons (Figure 4, A and A′ vs. B and B′). However, in the WT-FGFR1 neurons, the presence of nearby muscle did not lead to additional filopodial growth (unlike in GFP neurons). Thus the AI of filopodial distribution in WT-FGFR1 neurons near muscle cells was lower than that in GFP neurons (Figure 4E). In the TR-FGFR1 neurons, filopodial density remained low, and muscle cells induced no filopodia (Figure 4, C and C′), which again was evident as a lower AI of filopodial distribution than in GFP neurons (Figure 4E).

The low AI of filopodial distribution in TR-FGFR1–expressing neurons could occur by this mutant, nonsignaling form of the receptor having led to a diminution in the axon's response to muscle-derived bFGF. On the other hand, WT-FGFR1 expression in neurons could have globally elevated FGFR1 activity through autophosphorylation and enhanced basal filopodial assembly, thus masking endogenous FGFR1's response to muscle-derived bFGF. This explanation rests on the hypothesis that muscle-presented bFGF is capable of stimulating filopodia in spinal neurons, which was then tested.

First, we overexpressed bFGF in neurons. As shown in Figure 4, D and D′, axons of these neurons exhibited more filopodia, presumably through an autocrine stimulation of their FGFR1. However, their

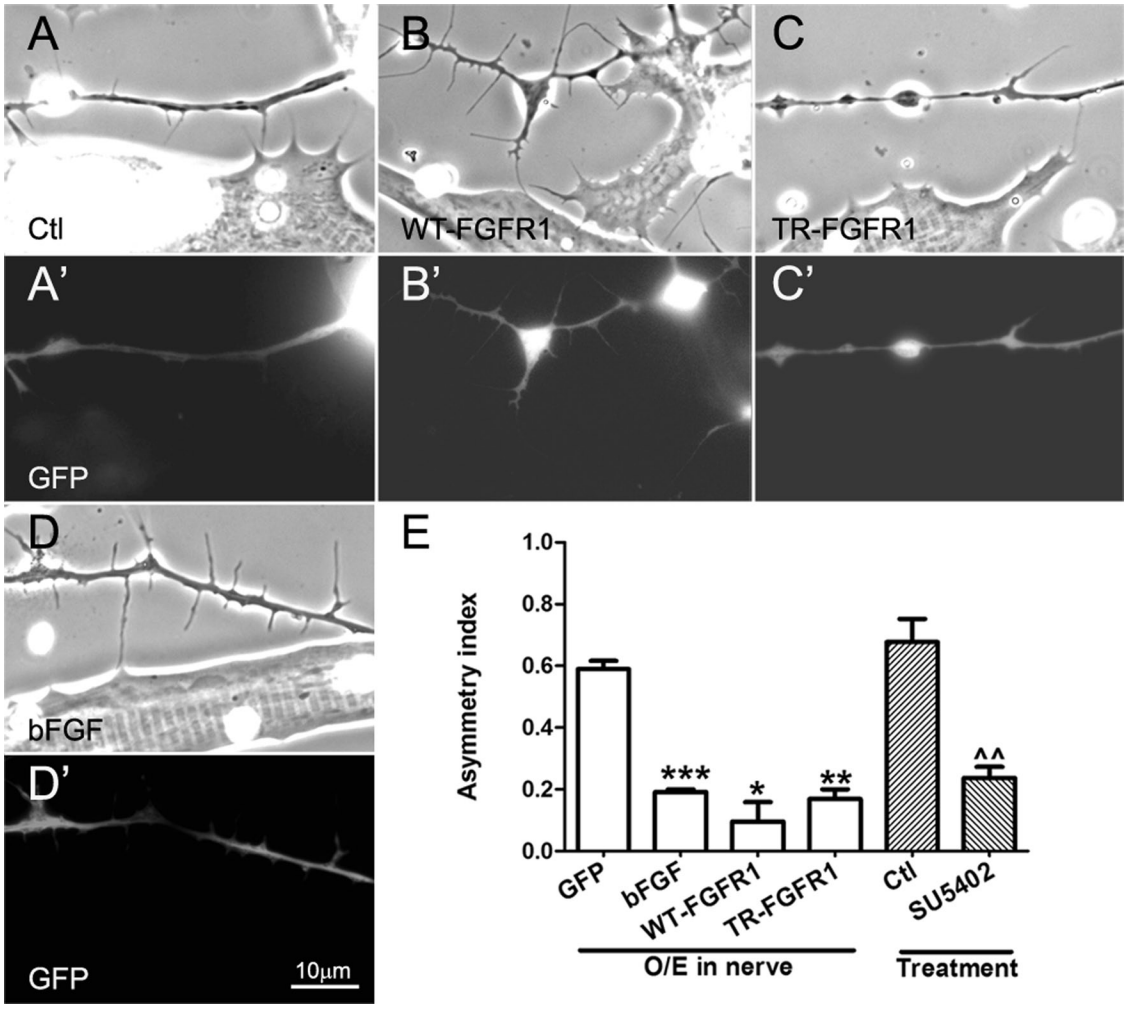

FIGURE 4: Regulation of axonal filopodial asymmetry by neuronal FGFR1 signaling. *Xenopus* spinal neurons expressing GFP (A, A′) or GFP and exogenous WT-FGFR1 (B, B′), TR-FGFR1 (C, C′), or bFGF (D, D′) were cocultured with normal muscle cells, and filopodia were examined in axons near muscle cells. Nerve–muscle cocultures treated with SU5402 (20 μM) were also compared with control cocultures (E). Relative to control GFP-expressing neurons (A, A′), neurons overexpressing WT-FGFR1 (B, B′) developed more filopodia, and those expressing TR-FGFR1 grew fewer filopodia (C, C′), but in these cases the preferential extension of filopodia toward muscle was less pronounced than it was in bFGF-overexpressing neuron–muscle cocultures (D, D′). (E) Quantification of these results. Axonal filopodial AI values in cocultures involving neurons expressing exogenous bFGF and two kinds of FGFR1 constructs, as well as SU5402 treatment, are shown. Numbers are mean ± SEM; *t* test, *$p < 0.05$, **$p < 0.01$, and ***$p < 0.001$ for comparisons of bFGF/FGFR1–expressing and control GFP neurons, and ^^$p < 0.01$ for comparison of untreated and SU5402 treated cocultures.

asymmetry due to muscle's presence was much lower than that seen in control GFP neurons (Figure 4E), much the same as in WT-FGFR1–expressing neurons. To address whether bFGF-FGFR1 signaling is physiologically relevant in regulating the asymmetric formation of axonal filopodia, the FGFR1-specific inhibitor SU5402 was added to normal nerve–muscle cocultures, and the results showed that SU5402 treatment reduced the axonal filopodial asymmetry by 60% (Figure 4E).

We next cocultured normal spinal neurons with muscle cells overexpressing hemagglutinin (HA)-tagged bFGF (with HA-tag linked to the C-terminus of bFGF). The overexpression was confirmed by the coexpression of GFP (Figure 5) and by labeling live cultures with anti-HA antibody. HA-bFGF was detected at AChR clusters in cells that expressed the exogenous protein, but no labeling was observed in cells expressing GFP only (unpublished data). When axons approached muscle cells overexpressing bFGF, they extended more filopodia from their muscle-facing side than the muscle-free side (Figure 5, B and B′, vs. the control GFP-expressing muscle, Figure 5, A and A′); significantly, the AI of filopodial distribution (Figure 5E) in these neurites was ~20% higher than that in axons near muscle cells expressing GFP alone.

As bFGF is a muscle-intrinsic protein (Figure 2), we wondered whether suppressing its expression would affect filopodial asymmetry in axons. To test this, normal spinal neurons were cocultured with muscle cells that were isolated from embryos injected with fluorescein-conjugated antisense-bFGF morpholino oligonucleotides (bFGF-MO) or control morpholino (Ctl-MO). The specificity of bFGF-MO was confirmed using HEK293 cells transfected with myc-tagged *Xenopus* bFGF plasmids: immunoblotting showed that the transfected cells expressed exogenous bFGF and that the introduction of *Xenopus* bFGF-specific morpholino, but not control morpholino, abolished the expression of the exogenous protein (unpublished

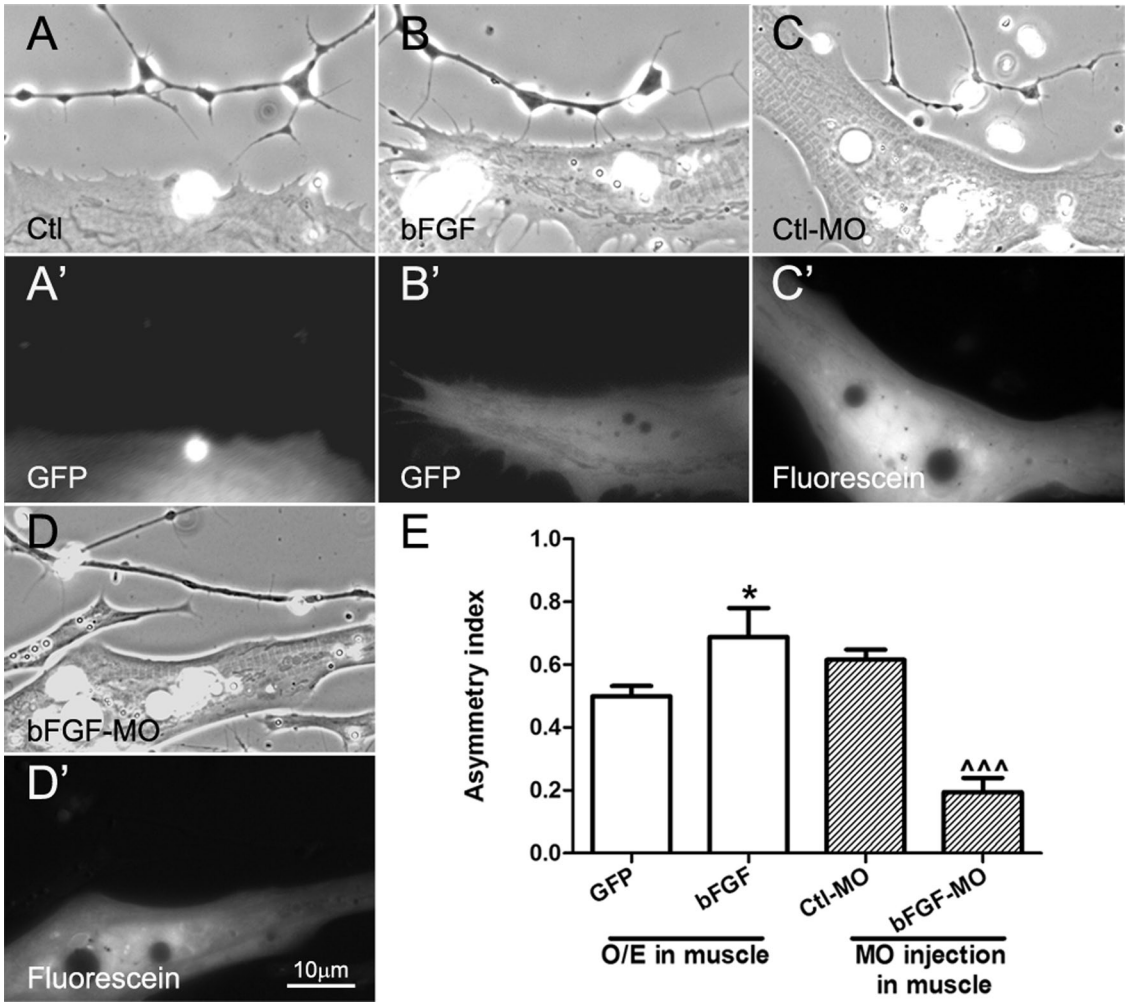

FIGURE 5: Effects of manipulating muscle bFGF expression on axonal filopodial asymmetry. Spinal neurons were cocultured with muscle cells isolated from embryos expressing GFP (A, A′), GFP plus exogenous bFGF (B, B′), control morpholinos (C, C′), or bFGF morpholinos (D, D′). Overexpression of bFGF in muscle led to enhanced filopodial asymmetry in neurons compared with that in cocultures using control GFP-expressing muscle. On the other hand, muscle cells bearing bFGF but not control morpholinos suppressed axonal filopodial asymmetry. (E) Quantification of these results. Values shown are mean ± SEM; *t* test, *$p < 0.05$ for comparisons of neurons near GFP- and GFP/bFGF–expressing muscle cells, and ^^^$p < 0.001$ for comparison of neurons near Ctl-MO– and bFGF-MO–injected muscle cells.

data). When axons grew near bFGF-MO–bearing muscle cells, the asymmetric filopodial extension toward muscle was reduced, in contrast to that seen near Ctl-MO–bearing muscle (Figure 5, D and D′ vs. C and C′). As shown in Figure 5E, the AI of axonal filopodial formation was reduced by ~70% in neurons cocultured with bFGF-MO muscle cells, suggesting that bFGF is a muscle-intrinsic molecule that causes the preferential extension of axonal filopodia in cocultures.

The function of neuronal FGFR1 signaling in NMJ formation

In rodent nerve–muscle cocultures, myopodia facilitate tight interactions between nerve and muscle (Uhm *et al.*, 2001). We previously found that suppression of myopodial assembly, through expression in *Xenopus* muscle of a "Rho-mutant" form of the protein p120 catenin (p120ctn), inhibited NMJ development, which was seen as a reduction in the clustering of muscle AChRs at early nerve–muscle contacts (Madhavan *et al.*, 2006). Here we monitored nerve-induced AChR aggregation in muscle to assess whether blocking filopodial assembly in spinal neurons affects synaptogenesis. Wild-type and mutant FGFR1 were expressed in *Xenopus* spinal neurons by mRNA injection, and the ability of these neurons to induce focal AChR aggregation in muscle was quantified.

Spinal neurons expressing GFP and wild-type or mutant FGFR1 were seeded on normal muscle cells, and 1-d-old cocultures were labeled for AChR clusters (Figure 6). Compared to GFP (Figure 6, A–C) and WT-FGFR1 neurons (Figure 6, D–F), neurons expressing TR-FGFR1 poorly induced AChR clustering at innervation sites (Figure 6, G–I). In the absence of nerve-induced AChR clustering, preexisting receptor hotspots persisted (Figure 6I, h.s.). Scoring nerve–muscle contacts with AChR clusters showed that neurons expressing TR-FGFR1 were ~25% less effective at establishing NMJs than those expressing GFP or WT-FGFR1 (Figure 6P). Thus a reduction in filopodial generation in axons through FGFR1 suppression is correlated with partial inhibition of NMJ formation as shown by muscle AChR clustering.

Next muscle cells were cultured from embryos injected with Ctl-MO (Figure 6, J–L) or bFGF-MO (Figure 6, M–O); in these cells AChR clustering was normal, as shown by the presence of preexisting receptor hotspots (Figure 6O). When normal neurons were seeded on

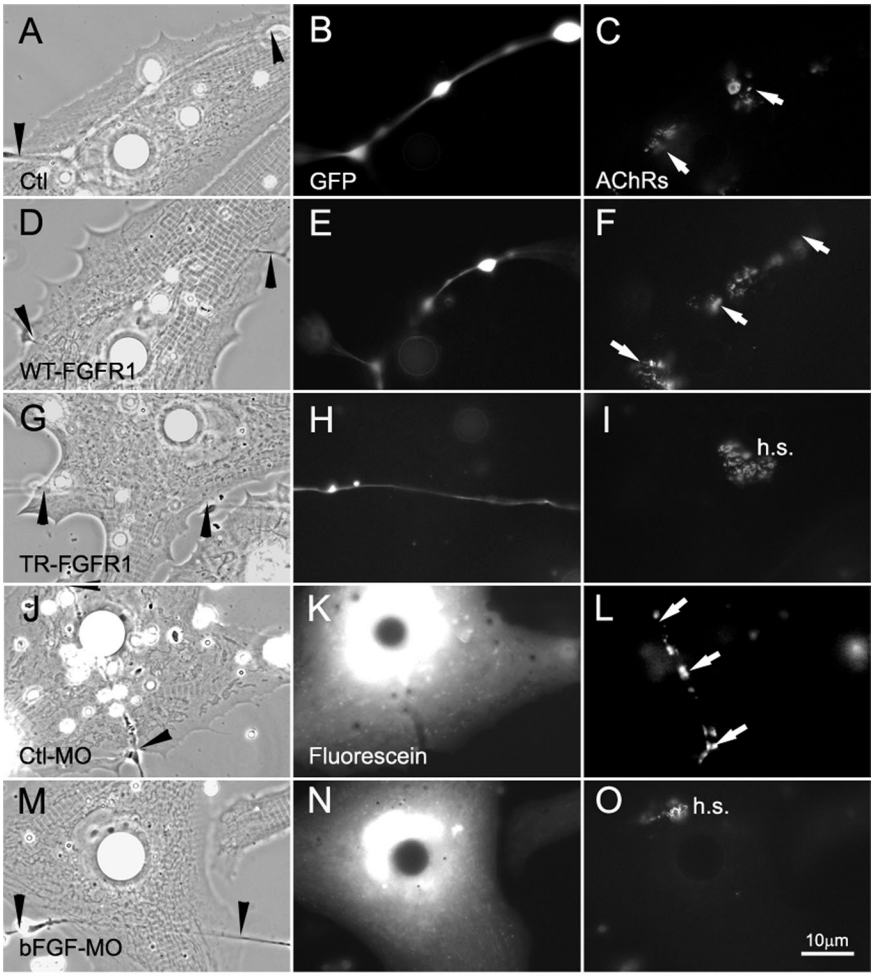

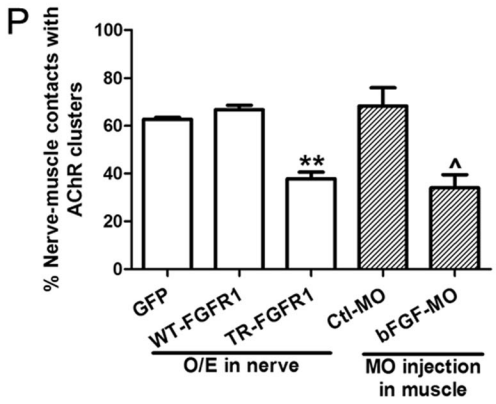

FIGURE 6: Regulation of NMJ assembly by FGF signaling. NMJ formation in cocultures with alterations in FGF signaling was assessed by AChR clustering, which was monitored by R-BTX labeling (right). (A–C) AChR clusters (C, arrows) were present along the nerve–muscle contact in the control nerve–muscle coculture. (D–F) Similar to the control, AChR clusters were detected at nerve–muscle contacts in cocultures involving WT-FGFR1–expressing spinal neurons (D–F). (G–I) Suppression of FGFR1 function in neurons through expression of TR-FGFR1–inhibited NMJ formation, as shown by the lack of AChR clusters associated with the nerve–muscle contact. In the absence of nerve-induced AChR clustering, preexistent AChR clusters in the cells (hotspots) persisted (I, h.s.). In these parts of the figure, GFP coexpressed in the neurons was used to mark the expression of exogenous proteins. (J–L) Expressing control morpholinos in muscle (shown by fluorescence in K) did not affect NMJ formation, but the expression of bFGF morpholino (M–O) suppressed NMJ assembly, seen here once again as a lack of AChR clustering at nerve–muscle contacts and the persistence of hotspots. (P) Quantification of data showing the mean ± SEM; *t* test, **$p < 0.01$ for comparisons of FGFR1-expressing and control GFP neurons and ^$p < 0.05$ for comparison of Ctl-MO– and bFGF-MO–injected muscle cells.

these cells and synaptic AChR clustering was quantified, the results showed that NMJ formation between spinal neurons and bFGF-MO–bearing muscle cells was decreased by ~40% compared with that with Ctl-MO–bearing muscle cells (Figure 6Q). In contrast, introduction of bFGF-MO into spinal neurons (which express low levels of bFGF; see Figure 2A) did not lead to a reduction in nerve-induced AChR clustering in muscle (unpublished data). These results suggest that muscle-derived bFGF, a regulator of axonal filopodial asymmetry, also contributes to NMJ formation.

DISCUSSION

In this study the interaction between nerve and muscle during the early stages of NMJ assembly was studied using molecular and cell biological approaches. We found the following. 1) Muscle cells enhanced the growth and stabilization of filopodia in approaching spinal neurons. 2) bFGF was expressed by and associated with the surface of muscle cells. 3) bFGF applied either exogenously or presented by muscle cells generated filopodia in spinal neurons. 4) FGFR1 signaling in neurons promoted the formation of filopodia. 5) Knocking down of bFGF in muscle by antisense morpholino injection reduced both axonal filopodial asymmetry and NMJ establishment. 6) Suppression of FGFR1 signaling in neurons reduced nerve-induced AChR clustering in muscle cells. On the basis of these results we propose that activation by muscle bFGF of neuronal FGFR1 enhances filopodial processes in spinal neurons, which promote interactions between nerve and muscle to facilitate NMJ establishment.

Filopodial processes enable cells to explore their environment and to initiate contacts with neighboring cells. Besides neuromuscular interactions (Ritzenthaler *et al.*, 2000; Uhm *et al.*, 2001; Madhavan *et al.*, 2006), recent studies have revealed that filopodia also promote synaptogenic interactions of central neurons (Arikkath and Reichardt, 2008; Yoshihara *et al.*, 2009; Heiman and Shaham, 2010). It is interesting to note that axonal filopodia emanate from varicosities (Figure 1) enriched in synaptic vesicles (as revealed by immunolabeling; unpublished data). Thus the generation of axonal filopodia is likely to be a prelude to presynaptic differentiation.

In this study, it was observed that filopodia were preferentially extended toward the muscle target in nerve–muscle cocultures, which was seen as a high AI value. Time-lapse imaging showed that this was at least partly due to increased stabilization of filopodia facing muscle. This asymmetry was observed even along thin axons (~1 μm in diameter), suggesting that muscle surface–bound factors or those that are released and deposited pericellularly by the

muscle, rather than a gradient of diffusible ones, are responsible for generating this difference. Our finding that bFGF plays a key role in regulating axonal filopodial asymmetry is consistent with this notion: it is well known that bFGF, through its binding to HSPG at the cell surface, has low diffusibility and tends to be sequestered at or near the cell perimeter (Gallagher and Turnbull, 1992). The AI of filopodial distribution in axons was lowered, however, following the activation or inactivation of FGFR1 in neurons (achieved through the overexpression of WT-FGFR1 or TR-FGFR1, respectively) or by the expression of excess bFGF in neurons. In contrast, overexpression of bFGF in muscle cells increased the AI of filopodial distribution in nearby axons and knocking down of bFGF in muscle reduced it. These findings suggest that activation of neuronal FGFR1 by muscle-derived bFGF promotes filopodial formation in spinal neurons. What additional factors from muscle control filopodial growth in neurons are currently unknown, but growth factors and other molecules secreted by and/or associated with the muscle surface could be tested in the future. For example, FGFs 7, 10, and 22 all can regulate presynaptic differentiation at the NMJ (Umemori *et al.*, 2004; Fox *et al.*, 2007) and, among these, FGF10 can also activate FGFR1 (Eswarakumar *et al.*, 2005); it would thus be of interest to investigate whether FGF10, by activating FGFR1, works together with and enhances the effect of bFGF or independently influences nerve–muscle interactions at a different stage of development.

We observed that the expression of inactive FGFR1 (TR-FGFR1) in neurons suppressed basal and muscle-dependent filopodial assembly and further led to a reduction in the ability of the neurons to induce muscle AChR clustering, a phenomenon also noted after bFGF knockdown in muscle. This suggests that neuronal filopodia facilitate synaptogenic nerve–muscle interactions, much like the myopodia induced by spinal neurons (Madhavan *et al.*, 2006). Of interest, overexpression of WT-FGFR1 in neurons, which elevated the overall density of filopodia, also lowered the AI of filopodial distribution in cocultures, but this did not inhibit NMJ assembly. Thus the presence of excess filopodia in these neurons could have enabled nerve to make sufficient contacts with muscle for the initiation of NMJ assembly, supporting the notion that a dynamic development of filopodia, rather than the preferential extension of filopodia toward muscle, is important for establishment of synaptogenic nerve–muscle contacts.

Dendritic filopodia in central neurons are now recognized to serve as precursors of postsynaptic dendritic spine apparatus in addition to their function in mediating axonal contact and interaction (Dailey and Smith, 1996; Ziv and Smith, 1996; Sekino *et al.*, 2007). This study on axonal filopodia has described a previously unappreciated function of bFGF in enhancing functional nerve–muscle interaction by triggering filopodial growth in spinal neurons. This adds to our earlier findings showing that bFGF promotes the clustering of SVs and mitochondria in neurons (Dai and Peng, 1995; Lee and Peng, 2008) and the aggregation of AChRs in muscle (Peng *et al.*, 1991a). More broadly, these studies support the view that FGFs are important synaptogenic factors that function in the PNS and the CNS: besides bFGF, FGFs 7, 10, and 22 have been found to promote presynaptic differentiation at the rodent NMJ (Umemori *et al.*, 2004; Fox *et al.*, 2007), and more recently FGFs 7 and 22 have been shown to regulate presynaptic differentiation at inhibitory and excitatory synapses, respectively, in central neurons (Terauchi *et al.*, 2010). Our results suggesting that FGFR1 signaling generates filopodia in spinal neurons could also be relevant in the CNS. FGFR1 is widely expressed in the brain (Gonzalez *et al.*, 1995), and it is activated by many FGFs (Eswarakumar *et al.*, 2005). By suppressing or boosting the activities of FGFR1 in central neurons, future studies could test whether these important signaling proteins, which regulate diverse cellular events, collaborate in mediating the assembly and/or remodeling of CNS synapses. A previous study reported that bFGF-coated beads induce axonal branching in cultured cortical neurons (Kalil *et al.*, 2000), and since axonal branching precedes the axon's interaction with postsynaptic target, this further illustrates the role of FGF family of growth factors in synaptic development.

In dorsal root ganglion neurons, local or bath application of the neurotrophin NGF induces filopodia via the activation of TrkA tyrosine kinase receptor and through PI3 kinase signaling and local F-actin remodeling (Gallo and Letourneau, 1998; Ketschek and Gallo, 2010). NGF promotes the formation of submicron-sized F-actin patches along the axon that dynamically undergo assembly and dissipation in seconds, with filopodia developing at a subset of these sites during the transition. In a recent study we found that, like myopodia (Madhavan *et al.*, 2006), axonal filopodia in *Xenopus* neurons are generated by signaling through the actin regulators p120ctn and Rho-family small GTPases (C. Chen, P. Li, R. Madhavan, and H. B. Peng, unpublished data). Together, these works suggest that axonal filopodia are formed in response to retrograde, target-derived stimuli via local kinase activation and F-actin dynamics.

MATERIALS AND METHODS

Reagents

The following reagents were purchased from the suppliers listed: recombinant human bFGF (R&D, Minneapolis, MN); SU5402 (Calbiochem, San Diego, CA); R-BTX (Molecular Probes; Eugene, OR); anti-bFGF rabbit polyclonal antibody (American Diagnostica, Stamford, CT); horseradish peroxidase (HRP)–conjugated secondary antibodies (Jackson Immuno Research Laboratories; West Grove, PA); and TX-100 and enhanced chemiluminescence (ECL) reagent West Pico (Pierce, Rockford, IL). Antisense bFGF-MO and Ctl-MO conjugated to fluorescein were from Gene Tools (Philomath, OR). *Xenopus* bFGF-MO has the sequence:5-GAGTTGTGATGCTCCCTGCCGCCAT-3, and Ctl-MO has 5-CCTCTTACCTCAGTTACAATTTATA-3.

Expression of exogenous proteins in *Xenopus* spinal neurons and muscle cells

Xenopus FGFR1 cDNA was a generous gift from Robert Friesel (Maine Medical Center Research Institute, Scarborough, ME); from this cDNA we generated HA-tagged, full-length FGFR1 (WT-FGFR1) and intracellular domain-truncated FGFR1 (TR-FGFR1) constructs. These constructs and one encoding GFP were subcloned into the pCS2+ vector, from which mRNAs were synthesized (after plasmid linearization) using SP6 polymerase with the mMESSAGE mMACHINE kit (Ambion, Austin, TX); bFGF cloned from a mouse heart cDNA library was HA tagged and subcloned into pCDNA3.1 vector for mRNA synthesis with T7 polymerase (again using the mMESSAGE mMACHINE kit). To express foreign proteins in neurons and muscle cells, mRNAs were injected into one cell in two- to four-stage *Xenopus* embryos using a Drummond Nanojet Oocyte Injector (Drummond Scientific, Broomall, PA). The FGFR1 and bFGF mRNAs were mixed with GFP mRNA before injection. GFP-positive embryos at stage 20–22 were selected, and nerve and muscle cultures and cocultures were prepared.

Xenopus nerve and muscle primary cultures

Primary cultures of *Xenopus* spinal neurons, myotomal muscle cells, and nerve–muscle cocultures were prepared as described

(Peng *et al.*, 1991b). Briefly, embryos at stage 20–22 were dissected, and neural tubes and myotomes were isolated, which were then dissociated in a Ca^{2+}/Mg^{2+}–free solution. Dissociated spinal neurons and muscle cells were plated separately on coverglass coated with entactin–collagen IV–laminin substrate (Upstate, Millipore, Billerica, MA) for obtaining pure nerve and muscle cultures. For generating cocultures, freshly isolated neurons were seeded onto 4- to 7-d-old muscle cultures and maintained for 1 d before use.

Visualization of bFGF localization, filopodial assembly, and NMJ formation

To investigate bFGF localization, live muscle cultures and nerve–muscle cocultures were labeled with anti-bFGF or control antibodies after staining with R-BTX (3 nM) to mark AChR clusters; FITC-conjugated secondary antibodies were used to detect the primary antibodies. Filopodial assembly in live pure nerve cultures and nerve–muscle cocultures was visualized in phase contrast; in cases in which exogenous proteins were introduced into neurons or muscle cells, GFP fluorescence was first used to check for protein expression. Filopodia that developed along the length of neurites in the two directions roughly perpendicular to growth on the substrate were monitored in all cases, and in nerve–muscle cocultures, filopodia were taken into account in neurite segments that were no more than 30 µm from muscle cells. All of the filopodia growing within selected segments of neurites were counted to calculate their densities (as number of filopodia/10-µm neurite length) and the asymmetry of filopodial distribution.

To study the effect of bFGF on filopodial assembly and to examine nerve–muscle synapse formation, pure nerve cultures or 1-d-old nerve–muscle cocultures were prepared in custom-made, sealed "live-chambers." Pure nerve cultures were exposed to bFGF (100 ng/ml) overnight. Nerve–muscle contacts were identified in phase contrast, and fluorescence microscopy was used to monitor the expression of exogenous proteins and AChR clusters in muscle. To quantify NMJ formation, nerve–muscle contacts in many separate coculture preparations were randomly chosen using phase contrast and checked for AChR clustering at innervation sites in muscle; from this the percentages of nerve–muscle contacts with AChR aggregates were calculated.

Immunoprecipitation and Immunoblotting

Xenopus embryonic myotomes and neural tubes were first dissociated into single cells with Ca^{2+}/Mg^{2+}–free Steinberg's solution and then harvested in SDS loading buffer. Extract of *Xenopus* whole embryos at stage 20–22 were prepared in modified RIPA buffer (25 mM HEPES, pH 7.4, 150 mM NaCl, 1 mM EDTA, 0.25% Na deoxycholate, 1% NP-40, 1 mM dithiothreitol and 1 mM phenylmethylsulfonyl fluoride [PMSF]). To obtain positive and negative controls for bFGF staining in immunoblotting assays, HEK293T cells were used that had been transfected with cDNAs encoding mouse bFGF or GFP (using Lipofectamine 2000). To monitor the activity of exogenous FGFR1 proteins, HEK293T cells were transfected with cDNAs encoding WT- and TR-FGFR1 constructs. In experiments in which protein phosphorylation was monitored, the activity of tyrosine phosphatases in cells was kept low by adding Na pervanadate (10 µM). Na pervanadate was prepared fresh before use by mixing 10 mM Na orthovanadate with 1.7% H_2O_2 at a 50:1 ratio and then diluted into culture medium (Madhavan *et al.*, 2005). Cells were lysed (30 min) in ice-cold IP buffer (25 mM HEPES, pH7.4, 150 mM NaCl, 1 mM EDTA, 1% Triton X-100) containing the protease inhibitor PMSF (1 mM) and Na pervanadate (1 mM); lysates were sonicated and then clarified by centrifugation. To 0.4- to 0.6-ml extracts, 1 to 2 µg of antibodies and 15 µl of protein A/G agarose slurry were added and mixed for 3 h at 4°C. Beads were spun down and washed thrice with the IP buffer before mixing in 30–50 µl of SDS–electrophoresis sample buffer; eluted proteins were separated by SDS–PAGE (10% gels) and transferred to polyvinylidene fluoride membranes for immunoblotting. Membranes were blocked with 4% bovine serum albumin and then stained with primary and HRP-conjugated secondary antibodies for ECL-based detection.

Microscopy and statistics

Cultures were examined using a Zeiss Axiovert 200M microscope equipped with a Zeiss AxioCamMR camera controlled by AxioVision Pel 4.5 software. Data are presented as mean ± SEM values; paired Student's *t* tests were carried out with Graphpad Prism statistical software.

ACKNOWLEDGMENTS

This investigation was supported by Hong Kong Research Grants Council Grant 662108 and Areas of Excellence Grant B-15/01-II. We thank Robert Friesel for the *Xenopus* FGFR1 cDNA and W. K. Wong for the gift of recombinant bFGF during this study.

REFERENCES

Amaya E, Musci TJ, Kirschner MW (1991). Expression of a dominant negative mutant of the FGF receptor disrupts mesoderm formation in *Xenopus* embryos. Cell 66, 257–270.

Arikkath J, Reichardt LF (2008). Cadherins and catenins at synapses: roles in synaptogenesis and synaptic plasticity. Trends Neurosci 31, 487–494.

Dai Z, Peng HB (1995). Presynaptic differentiation induced in cultured neurons by local application of basic fibroblast growth factor. J Neurosci 15, 5466–5475.

Dai Z, Peng HB (1998). A role of tyrosine phosphatase in acetylcholine receptor cluster dispersal and formation. J Cell Biol 141, 1613–1624.

Dailey ME, Smith SJ (1996). The dynamics of dendritic structure in developing hippocampal slices. J Neurosci 16, 2983–2994.

Eswarakumar VP, Lax I, Schlessinger J (2005). Cellular signaling by fibroblast growth factor receptors. Cytokine Growth Factor Rev 16, 139–149.

Feng Z, Ko CP (2008). Schwann cells promote synaptogenesis at the neuromuscular junction via transforming growth factor-beta1. J Neurosci 28, 9599–9609.

Fertuck HC, Salpeter MM (1976). Quantitation of junctional and extrajunctional acetylcholine receptors by electron microscope autoradiography after 125I-alpha-bungarotoxin binding at mouse neuromuscular junctions. J Cell Biol 69, 144–158.

Fitzsimonds RM, Poo MM (1998). Retrograde signaling in the development and modification of synapses. Physiol Rev 78, 143–170.

Fox MA *et al.* (2007). Distinct target-derived signals organize formation, maturation, and maintenance of motor nerve terminals. Cell 129, 179–193.

Fox MA, Umemori H (2006). Seeking long-term relationship: axon and target communicate to organize synaptic differentiation. J Neurochem 97, 1215–1231.

Gallagher JT, Turnbull JE (1992). Heparan sulphate in the binding and activation of basic fibroblast growth factor. Glycobiology 2, 523–528.

Gallo G, Letourneau PC (1998). Localized sources of neurotrophins initiate axon collateral sprouting. J Neurosci 18, 5403–5414.

Gallo G, Letourneau PC (2004). Regulation of growth cone actin filaments by guidance cues. J Neurobiol 58, 92–102.

Gerrow K, El-Husseini A (2006). Cell adhesion molecules at the synapse. Front Biosci 11, 2400–2419.

Gonzalez AM, Berry M, Maher PA, Logan A, Baird A (1995). A comprehensive analysis of the distribution of FGF-2 and FGFR1 in the rat brain. Brain Res 701, 201–226.

Heiman MG, Shaham S (2010). Twigs into branches: how a filopodium becomes a dendrite. Curr Opin Neurobiol 20, 86–91.

Kalil K, Szebenyi G, Dent EW (2000). Common mechanisms underlying growth cone guidance and axon branching. J Neurobiol 44, 145–158.

Ketschek A, Gallo G (2010). Nerve growth factor induces axonal filopodia through localized microdomains of phosphoinositide 3-kinase

activity that drive the formation of cytoskeletal precursors to filopodia. J Neurosci 30, 12185–12197.
Kim N, Stiegler AL, Cameron TO, Hallock PT, Gomez AM, Huang JH, Hubbard SR, Dustin ML, Burden SJ (2008). Lrp4 is a receptor for agrin and forms a complex with MuSK. Cell 135, 334–342.
Kummer TT, Misgeld T, Sanes JR (2006). Assembly of the postsynaptic membrane at the neuromuscular junction: paradigm lost. Curr Opin Neurobiol 16, 74–82.
Kusakabe M, Masuyama N, Hanafusa H, Nishida E (2001). *Xenopus* FRS2 is involved in early embryogenesis in cooperation with the Src family kinase Laloo. EMBO Rep 2, 727–735.
Lee CW, Peng HB (2006). Mitochondrial clustering at the vertebrate neuromuscular junction during presynaptic differentiation. J Neurobiol 66, 522–536.
Lee CW, Peng HB (2008). The function of mitochondria in presynaptic development at the neuromuscular junction. Mol Biol Cell 19, 150–158.
Madhavan R, Peng HB (2005). Molecular regulation of postsynaptic differentiation at the neuromuscular junction. IUBMB Life 57, 719–730.
Madhavan R, Zhao XT, Reynolds AB, Peng HB (2006). Involvement of p120 catenin in myopodial assembly and nerve-muscle synapse formation. J Neurobiol 66, 1511–1527.
Madhavan R, Zhao XT, Ruegg MA, Peng HB (2005). Tyrosine phosphatase regulation of MuSK-dependent acetylcholine receptor clustering. Mol Cell Neurosci 28, 403–416.
Nishimune H, Sanes JR, Carlson SS (2004). A synaptic laminin-calcium channel interaction organizes active zones in motor nerve terminals. Nature 432, 580–587.
Peng HB, Baker LP, Chen Q (1991a). Induction of synaptic development in cultured muscle cells by basic fibroblast growth factor. Neuron 6, 237–246.
Peng HB, Baker LP, Chen Q (1991b). Tissue culture of *Xenopus* neurons and muscle cells as a model for studying synaptic induction. Methods Cell Biol 36, 511–526.
Ritzenthaler S, Suzuki E, Chiba A (2000). Postsynaptic filopodia in muscle cells interact with innervating motoneuron axons. Nat Neurosci 3, 1012–1017.
Sanes JR, Lichtman JW (2001). Induction, assembly, maturation and maintenance of a postsynaptic apparatus. Nat Rev Neurosci 2, 791–805.
Sekino Y, Kojima N, Shirao T (2007). Role of actin cytoskeleton in dendritic spine morphogenesis. Neurochem Int 51, 92–104.
Szebenyi G, Dent EW, Callaway JL, Seys C, Lueth H, Kalil K (2001). Fibroblast growth factor-2 promotes axon branching of cortical neurons by influencing morphology and behavior of the primary growth cone. J Neurosci 21, 3932–3941.
Terauchi A, Johnson-Venkatesh EM, Toth AB, Javed D, Sutton MA, Umemori H (2010). Distinct FGFs promote differentiation of excitatory and inhibitory synapses. Nature 465, 783–787.
Uhm CS, Neuhuber B, Lowe B, Crocker V, Daniels MP (2001). Synapse-forming axons and recombinant agrin induce microprocess formation on myotubes. J Neurosci 21, 9678–9689.
Umemori H, Linhoff MW, Ornitz DM, Sanes JR (2004). FGF22 and its close relatives are presynaptic organizing molecules in the mammalian brain. Cell 118, 257–270.
Yoshihara Y, De Roo M, Muller D (2009). Dendritic spine formation and stabilization. Curr Opin Neurobiol 19, 146–153.
Zhang B, Luo S, Wang Q, Suzuki T, Xiong WC, Mei L (2008). LRP4 serves as a coreceptor of agrin. Neuron 60, 285–297.
Ziv NE, Smith SJ (1996). Evidence for a role of dendritic filopodia in synaptogenesis and spine formation. Neuron 17, 91–102.